J Syst Sci Complex (2021) 34: 3–20

Non-Uniform Doo-Sabin Subdivision Surface via Eigen Polygon*

ALAM Md Nur · LI Xin

DOI: 10.1007/s11424-020-9264-z
Received: 17 September 2019

Abstract This paper constructs a new non-uniform Doo-Sabin subdivision scheme via eigen polygon. The authors proved that the limit surface is always convergent and is G^1 continuous for any valence and any positive knot intervals under a minor assumption, that λ is the second and third eigenvalues of the subdivision matrix. And then, a million of numerical experiments are tested with randomly selecting positive knot intervals, which verify that our new subdivision scheme satisfies the assumption. However this is not true for the other two existing non-uniform Doo-Sabin schemes in Sederberg, et al. (1998), Huang and Wang (2013). In additional, numerical experiments indicate that the quality of the new limit surface can be improved.

Keywords Doo-Sabin, non-uniform, splines, subdivision.

1 Introduction

Subdivision is a powerful technique for computer aided geometrical design (CAGD) to generate high quality surfaces in a simple and stable way[1, 2]. Given a control grid, a subdivision scheme defines the rule to add new vertices as linear combinations of old ones and meanwhile to keep or change the locations of old vertices in each step. Repeating the process leads to a limit subdivision curve or surface. Approximating subdivision can be regarded as the generalization of the spline representation to arbitrary topology[1], such as Doo-Sabin subdivision[3], Catmull-Clark subdivision[4], Loop subdivision[5], $\sqrt{3}$-subdivision[6], 4-8 subdivision[7, 8], and Quad/triangle subdivision[9, 10]. The other classes of subdivision schemes are interpolatory, such as the four-point curve subdivision scheme[11], Butterfly scheme[12, 13], interpolatory subdivision for quadrilateral nets[14–16], interpolatory $\sqrt{3}$ and $\sqrt{2}$ subdivision[17, 18], interpolatory subdivision from approximating subdivision[19–22]. Subdivision surfaces are also attractive in

ALAM Md Nur · LI Xin
School of Mathematical Sciences, University of Science and Technology of China, Hefei 230026*, China.*
Email: lixustc@ustc.edu.cn.

*This research was supported by the National Natural Science Foundation of China under Grant No. 61872328, SRF for ROCS SE, and the Youth Innovation Promotion Association CAS, CAS-TWAS president's fellowship program.
◇ *This paper was recommended for publication by Editor-in-Chief GAO Xiao-Shan.*

isogeometric analysis (IGA), which directly performs numerical simulation based on the models from CAD[23–27]. Subdivision-based local refinement and its application in IGA have been studied for both Catmull-Clark subdivision[28, 29] and Loop subdivision[30]. In order to construct the NURBS-compatible subdivision scheme, [32] firstly introduces the non-uniform parameterization into the subdivision and later this issue is improved in [2, 31, 33–36].

In the paper[32], quadratic and cubic non-uniform recursive subdivision surfaces (NURSSes) are constructed. However, Qin et al.[37] point out that the quadratic NURSSes converge only when $n \leq 12$, and may diverge when $n > 12$. [33] constructs a non-uniform Doo-Sabin subdivision scheme by combining the non-uniform biquadratic B-spline and Catmull-Clark-variant Doo-Sabin subdivision (CCVDS), which is called NURDSes. The paper concludes that the scheme is G^1 for any valence $n, 3 \leq n \leq 30$ extraordinary faces. However, our experiments find out that the scheme is G^1 for the extraordinary faces with only one variable knot interval but it is only G^0 with two or more variable knot intervals.

This paper generalizes the non-unform biquadratic B-spline to arbitrary topology via eigen polygon, which can also be regarded as a generalization of CCVDS to non-uniform knot intervals. Unlike the existing schemes in [32, 33], the subdivision scheme in the present paper is proved to be G^1 for any positive knot intervals and any valence under a minor assumption. Also, the new scheme produces better quality limit surfaces. In summary, the main features of the paper include:

1) The new subdivision scheme generalizes non-uniform biquadratic B-spline to arbitrary topology;

2) The subdivision surface is proved to be always convergent and to be G^1-continuous under a minor assumption, which are stated in Theorems 4.1 and 4.2. To the authors' best knowledge, this is the minimum assumption for proving G^1-continuous in non-uniform case.

3) The numerical experiments indicate that the limit surface is G^1 and the limit surface of the present paper has better geometric quality than the two existing non-uniform Doo-Sabin subdivision schemes in [32, 33].

The rest of the paper is organized as following. Section 2 briefly discusses the background for the paper, including knot intervals, Doo-Sabin subdivision, Catmull-Clark-variant Doo-Sabin subdivision and non-uniform biquadratic B-spline refinement rules. Section 3 constructs the non-uniform Doo-Sabin subdivision via eigen polygon. In Section 4, we propose the comparison of new subdivision scheme with the existing two subdivision schemes on the continuity and shape quality. The last section includes conclusion as well as future work.

2 Problem Statement

All the non-uniform Doo-Sabin subdivision schemes try to generalize the non-uniform biquadratic B-spline representation to arbitrary topology. In this section, we review the biquadratic B-splines, Doo-Sabin subdivision scheme and the basic framework to construct the non-uniform Doo-Sabin subdivision scheme.

2.1 Non-Uniform Bi-Quadratic B-Spline Surface

A non-uniform biquadratic B-spline surface is defined in terms of a control grid $\{P_{i,j}\}$ that is topological a rectangular grid (see Figure 1 (a)). Each control point $P_{i,j}$ is assigned with a horizonal non-negative knot interval d_i and a vertical non-negative knot interval e_j, where each row or column of control grid shares with the same knot interval d_i or e_j. The non-uniform biquadratic B-spline surface can be defined as the limit process of knot splitting, i.e., inserting the midpoint knot for any two neighbor knots. In the following, all the subscripts are defined in terms of the module of the valence of the vertex.

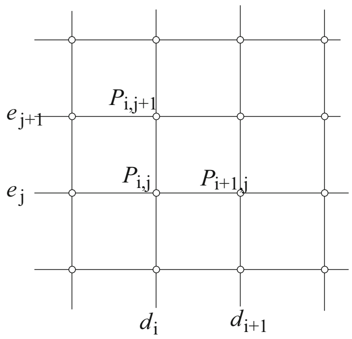

(a) Knot interval for a TP grid

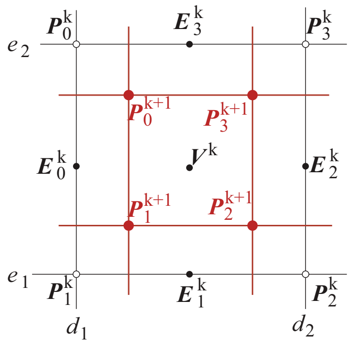

(b) Geometric rule

Figure 1 Define a non-uniform bi-quadratic B-spline surface in terms of knot splitting

As illustrated in Figure 1 (b), given a level k face with control points $P_i^k, i = 0, 1, 2, 3$ and knot intervals d_1, d_2, e_1, e_2, one round of knot insertion computes four face points P_i^{k+1} for the face. Denote

$$E_0^k = \frac{e_1 P_0^k + e_2 P_1^k}{e_1 + e_2}, \quad E_2^k = \frac{e_1 P_3^k + e_2 P_2^k}{e_1 + e_2},$$
$$E_1^k = \frac{d_2 P_1^k + d_1 P_2^k}{d_1 + d_2}, \quad E_3^k = \frac{d_2 P_0^k + d_1 P_3^k}{d_1 + d_2},$$

and

$$V^k = \frac{d_2(e_1 + e_2)E_0^k + e_2(d_1 + d_2)E_1^k + d_1(e_1 + e_2)E_2^k + e_1(d_1 + d_2)E_3^k}{2(d_1 + d_2)(e_1 + e_2)}, \tag{1}$$

then $P_i^{k+1} = \frac{V^k + E_i^k + E_{i-1}^k + P_i^k}{4}, i = 0, 1, 2, 3.$

2.2 Doo-Sabin Subdivision Scheme

The Doo-Sabin subdivision scheme and Catmull-Clark-variant Doo-Sabin subdivision scheme are generalizations of uniform biquadratic B-splines to arbitrary topological control grids. The topological rule for the schemes can be considered as an iterative procedure that takes a mesh as input and generates a new mesh based on the steps below.

- For each vertex of each face, generate a new point as the linear combination of the vertices of the face;
- For each valence n face, connect the new points that have been generated for each vertex of the face to form a new valence n face;
- For each valence n vertex, connect the new points that have been generated for the faces that are adjacent to this vertex to form a valence n face;
- For each edge, connect the new points that have been generated for the faces that are adjacent to this edge to form a valence 4 face.

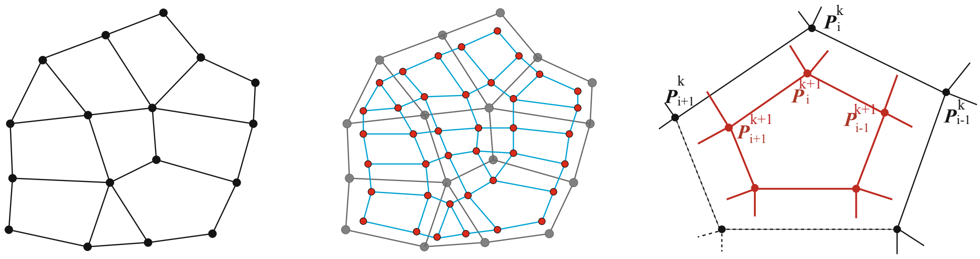

initial grid (b) topological rule (c) geometric rule

Figure 2 The rules for Doo-Sabin subdivision

The geometric rules of Doo-Sabin subdivision and Catmull-Clark-variant Doo-Sabin subdivision can be formalized in the similar way. For a valence n face in level k with vertices P_i^k, $i = 0, 1, \cdots, n-1$, after subdivision, a new valence n face with vertices P_i^{k+1}, $i = 0, 1, \cdots, n-1$ are computed. Each vertex P_i^{k+1} is a linear combination of the vertices P_i^k,

$$P_i^{k+1} = \sum_{j=0}^{n-1} \omega_{i,j} P_j^k. \tag{2}$$

The weights $\omega_{i,j}$ in the equation (2) have two forms. The first scheme is called Doo-Sabin subdivision scheme[3], where the weights $\omega_{i,j}$ are

$$\omega_{i,j} = \begin{cases} \dfrac{n+5}{4n}, & i = j; \\ \dfrac{3 + 2\cos(\frac{2(j-i)\pi}{n})}{4n}, & \text{else.} \end{cases} \tag{3}$$

The other possible scheme is called Catmull-Clark-variant Doo-Sabin subdivision scheme[4], where the weights are

$$\omega_{i,j} = \begin{cases} \dfrac{1}{2} + \dfrac{1}{4n}, & i = j; \\ \dfrac{1}{8} + \dfrac{1}{4n}, & |i-j| = 1; \\ \dfrac{1}{4n}, & \text{else.} \end{cases} \tag{4}$$

2.3 Non-Uniform Doo-Sabin Subdivision Scheme

The topological rule for the non-uniform Doo-Sabin subdivision is exactly same as that for Doo-Sabin subdivision. However in the situation of arbitrary topology, the valence of the vertex can be different from 4, so we can not define the two directional knot intervals as bi-quadratic B-splines. For a non-uniform Doo-Sabin surface, each vertex is assigned a non-negative knot interval (possibly different) for each edge incident to it, i.e., each valence n vertex is assigned with n knot intervals. Referring to Figure 3 (a), for the control grid of the first level, the notation $d^0_{i,j}$ indicates the knot interval for the vertex P_i along the edge P_iP_j. And $d^k_{i,j}$ denotes the knot interval for the vertex P_i along the k-th edge encountered when rotating the edge P_iP_j counter-clockwise. After subdivision, the new knot intervals, $\overline{d^k_{i,j}}$ will be specified as follows[32],

$$\overline{d^0_{i,i+1}} = \overline{d^{-1}_{i,i-1}} = d^0_{i,i+1}, \quad \overline{d^0_{i,i-1}} = \overline{d^1_{i,i+1}} = d^0_{i,i-1}. \tag{5}$$

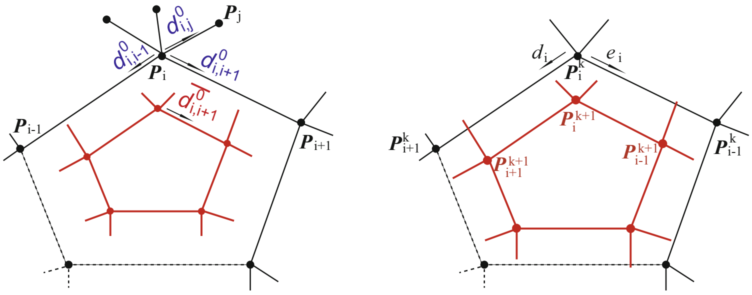

(a) New knot intervals (b) Notation in this paper

Figure 3 The notations for the knot intervals

Given a face with vertices P^0_i, $i = 0, 1, \cdots, n-1$, the geometric rule is only associated with the knot intervals $d^0_{i,i+1}$ and $d^0_{i,i-1}$. For simplicity, we denote the knot intervals $d_i = d^0_{i,i+1}$ and $e_i = d^0_{i,i-1}$ as illustrated in Figure 3. According to the new knot intervals rule, the knot intervals are invariant to the level k. Denote the vertices of the face in level k to be P^k_i. Defining an $n\times 3$ matrix $\boldsymbol{P}^k = [P^k_0, P^k_1, \cdots, P^k_{n-1}]^{\mathrm{T}}$ and $\boldsymbol{P}^{k+1} = [P^{k+1}_0, P^{k+1}_1, \cdots, P^{k+1}_{n-1}]^{\mathrm{T}}$, then the refinement rule can be written into a matrix form as $\boldsymbol{P}^{k+1} = M^k\boldsymbol{P}^k$, where M^k is an $n\times n$ matrix, whose element $M_{i,j}$ is a function of the knot intervals and the valence n. It is easy to see that the matrix M^k is stationary. Thus, we denote M^k as M in the following.

The scheme in [32] tries to combine the non-uniform biquadratic B-spline refinement rule and Doo-Sabin subdivision scheme,

$$P^{k+1}_i = \frac{P+P^k_i}{2} + \frac{d_{i+1}e_{i+3}+e_{i-1}d_{i-3}}{8\sum_{j=0}^{n-1} d_{j-1}e_{j+1}}\left(-nP^k_i + \sum_{j=0}^{n-1}\left(1+2\cos\left(\frac{2(i-j)\pi}{n}\right)\right)P^k_j\right), \tag{6}$$

where

$$P = \frac{\sum_{j=0}^{n-1} d_{j-1}e_{j+1}P^k_j}{\sum_{j=0}^{n-1} d_{j-1}e_{j+1}}.$$

The scheme in [33] tries to combine the non-uniform biquadratic B-spline refinement rule and Catmull-Clark-variant Doo-Sabin scheme,

$$P_i^{k+1} = \frac{N + E_i^k + E_{i-1}^k + P_i^k}{4}, \tag{7}$$

where $E_i^k = \frac{d_i P_{i+1}^k + e_{i+1} P_i^k}{d_i + e_{i+1}}$, $N = \frac{\sum_{j=0}^{n-1} c_j P_j^k}{\sum_{j=0}^{n-1} c_j}$ and

$$c_i = \frac{1}{2}\left(\prod_{j=0}^{n-1} d_j + \prod_{j=0}^{n-1} e_j\right) + \sum_{m=1}^{n-1}\left(\prod_{j=1}^{m} e_{i+j} \prod_{j=m}^{n-1} d_{i+j}\right). \tag{8}$$

3 Non-Uniform Doo-Sabin Subdivision via Eigen Polygon

This section provides our new non-uniform recursive Doo-Sabin subdivision via eigen polygon.

3.1 The Basic Idea of Eigen Polygon

Instead of defining the subdivision scheme by combining the Doo-Sabin subdivision and bi-quadratic B-spline refinement rule in a heuristic way, the present paper tries to define a polygon in the plane, for which the polygon after subdivision is only a scale and translation of the given polygon. And then a subdivision matrix can be constructed by satisfying the requirement. Under such construction, we can guarantee that the subdivision matrix has two identical eigenvalues.

Definition 3.1 Polygon $\widehat{\boldsymbol{P}}^0 \in R^2$ is an Eigen polygon of matrix M if there exist $\widehat{V} \in \mathbb{R}^2$ and $\lambda \in \mathbb{R}$ such that

$$\widehat{\boldsymbol{P}}^1 = M\widehat{\boldsymbol{P}}^0 = \boldsymbol{I}\widehat{V} + \lambda(\widehat{\boldsymbol{P}}^0 - \boldsymbol{I}\widehat{V}), \tag{9}$$

where M is a $n \times n$ matrix whose rows sum to one, $\boldsymbol{I}$ is a $n \times 1$ vector of 1's and $\widehat{\boldsymbol{P}}^1$ and $\widehat{\boldsymbol{P}}^0$ are n-element column vectors.

Remark 3.2 We can see that if the eigen polygon $\widehat{\boldsymbol{P}}^0$ exists, then

$$M(\widehat{\boldsymbol{P}}^0 - \boldsymbol{I}\widehat{V}) = M\widehat{\boldsymbol{P}}^0 - \boldsymbol{I}\widehat{V} = \lambda(\widehat{\boldsymbol{P}}^0 - \boldsymbol{I}\widehat{V}),$$

i.e., λ is the eigenvalue of the subdivision matrix M and x-coordinate and y-coordinate of $\widehat{\boldsymbol{P}}^0 - \boldsymbol{I}\widehat{V}$ correspond the two eigenvectors. This suggests that M will have an eigen polygon if M has two identical eigen values.

Remark 3.3 Although the basic idea of eigen polygon is similar as that in [35], but there is one key difference. For the eigen polygon, the new vertices are linear combination of all the vertices but the face or edge points in [35] are written into a bi-linear form. We solve the problem by adding a temporary point $\widehat{V}$ into the combination and compute the coefficients in the similar way.

3.2 Eigen Polygon for CCVDS and Non-Uniform Biquadratic B-Spline Refinement Rule

As the Catmull-Clark-variant Doo-Sabin subdivision and non-uniform biquadratic B-spline are G^1, so there are two identical eigenvalues for the corresponding subdivision matrix. We can compute the associated eigen polygon.

Catmull-Clark-variant Doo-Sabin eigen polygon A Catmull-Clark-variant Doo-Sabin refinement matrix has an eigen polygon

$$\widehat{P}_i^0 = \left(\cos\left(\frac{2i\pi}{n}\right), \sin\left(\frac{2i\pi}{n}\right)\right), \quad i = 0, 1, \cdots, n-1 \tag{10}$$

with $\lambda = \frac{1}{4} + \frac{1}{2}\cos^2(\frac{\pi}{n})$ and $\widehat{V} = (0, 0)$. In Figure 4, we show the Catmull-Clark-variant Doo-Sabin eigen polygon for valance 3, 5 and 6.

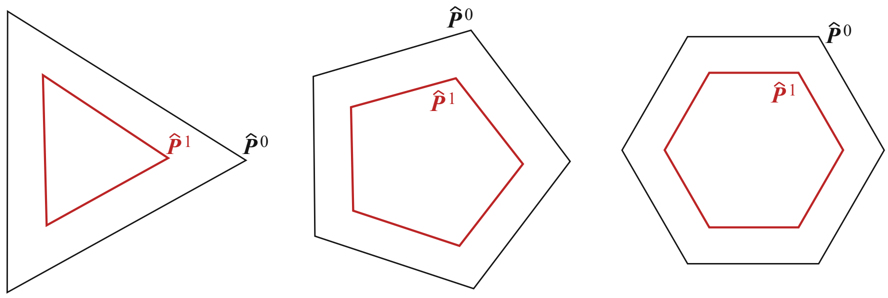

Figure 4 Catmull-Clark-variant Doo-Sabin eigen polygon

Non-uniform biquadratic B-spline eigen polygon For the non-uniform biquadratic B-splines, the knot intervals for d_i and e_i cannot be chosen arbitrarily. Actually, $d_i = e_{i-1}$. And then, the associated refinement matrix can also be constructed from the eigen polygon, which has the vertices

$$\widehat{P}_0^0 = (-1, -1), \quad \widehat{P}_1^0 = (1, -1), \quad \widehat{P}_2^0 = (1, 1), \quad \widehat{P}_3^0 = (-1, 1) \tag{11}$$

with $\lambda = \frac{1}{2}$ and $\widehat{V} = (\frac{d_0 - d_2}{d_0 + d_2}, \frac{d_1 - d_3}{d_1 + d_3})$. In the Figure 5, we shown the non-uniform biquadratic B-spline eigen polygon with different knot intervals.

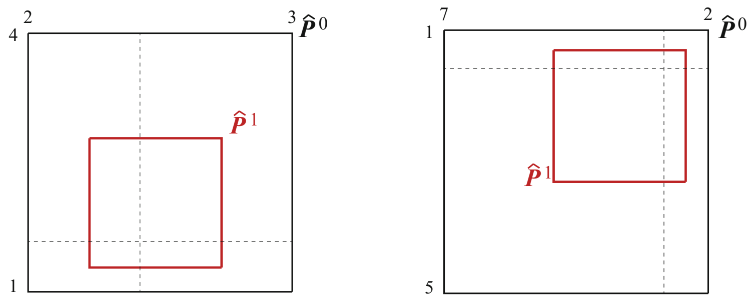

Figure 5 Non-uniform biquadratic B-spline Eigen polygon

3.3 Define the Subdivision Rule from Eigen Polygon

In this section, we define the subdivision matrix M with the eigen polygon idea. Since the rows of M express the combinations of the new vertices from the old ones, so the desired subdivision scheme that combines the Catmull-Clark-variant Doo-sabin refinement and non-uniform biquadratic B-spline refinement rule is equivalent to define the subdivision matrix that satisfy the following three requirements.

- The eigen polygon must specialize to Catmull-Clark-variant Doo-Sabin eigen polygon if the knot intervals are all equal;
- The eigen polygon must specialize to non-uniform biquadratic B-spline eigen polygon when the valence is 4 with the B-spline knot intervals;
- M must satisfy the requirement of eigen polygon;

We first explain how to design an eigen polygon for a valence-n face with the knot intervals d_i and e_i, where the points $\widehat{\boldsymbol{P}}_i^0$ are functions of n, d_i and e_i. The simplest way to define the eigen polygon is using the regular n-polygon because both non-uniform biquadratic B-spline Eigen polygon and Catmull-Clark-variant Doo-Sabin eigen polygon are regular n-polygons, as shown in Figure 6. Equation (9) also involves λ and $\widehat{V}$, so we begin by finding equations for λ and $\widehat{V}$ that specialize to the non-uniform biquadratic B-spline and Catmull-Clark-variant Doo-Sabin cases. Here we set $\lambda = \frac{1}{4} + \frac{1}{2}\cos^2(\frac{\pi}{n})$ and let $\widehat{V} = \sum_{i=0}^{n-1} \alpha_i \widehat{E}_i^0$, where $\alpha_i = \frac{(d_i+e_{i+1})(d_{i-1}+e_{i+2})}{\sum_{i=0}^{n-1}(d_i+e_{i+1})(d_{i-1}+e_{i+2})}$ and $\widehat{E}_i^0 = \frac{d_i\widehat{P}_{i+1}^0+e_{i+1}\widehat{P}_i^0}{d_i+e_{i+1}}$.

Remark 3.4 There are many degrees of freedoms to define the eigen polygon and $\widehat{V}$. We tried several other possible ways to define the eigen polygon and we find that the final shape qualities are similar. So in the present paper, we choose the simplest way to define the eigen polygon: The regular n-polygon. For the point $\widehat{V}$, the reason to choose such weights because we want the point $\widehat{V}$ always lies in the interior of $\widehat{\boldsymbol{P}}_i^0$ and each quadrilateral $\widehat{V}\widehat{E}_{i-1}^0\widehat{P}_i^0\widehat{E}_i^0$ is a convex quadrilateral, which can be used to prove that the subdivision is always convergent for any non-negative knot intervals in Theorem 4.1.

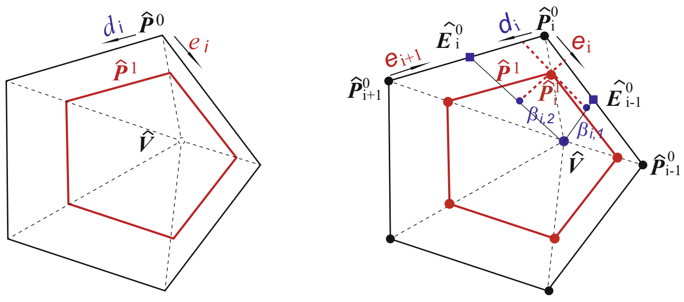

(a) Eigen polygon (b) Define the subdivision rule

Figure 6 Eigen polygon for the new non-uniform Doo-Sabin subdivision surface and we define the subdivision rule in terms of the eigen polygon

We now discuss how to create a refinement matrix M for which $\widehat{\boldsymbol{P}}^0$ is an eigen polygon. From the definition of the eigen polygon, we have

$$\widehat{P}_i^1 = \widehat{V} + \lambda(\widehat{P}_i^0 - \widehat{V}). \tag{12}$$

To devise a subdivision rule, we make the assumption that $\widehat{P}_i^1$ is the bi-linear combination of $\widehat{V}$, E_{i-1}^0, E_i^0 and $\widehat{P}_i^0$ with the weights β_i^1 and β_i^2, i.e,

$$\widehat{P}_i^1 = (1-\beta_i^1)(1-\beta_i^2)\widehat{V} + \beta_i^1(1-\beta_i^2)\widehat{E}_{i-1}^0 + (1-\beta_i^1)\beta_i^2\widehat{E}_i^0 + \beta_i^1\beta_i^2\widehat{P}_i^0. \tag{13}$$

The weights β_i^1 and β_i^2 can be solved via the following method. Denote $v_1 = \widehat{P}_i^1 - \widehat{V}$, $v_2 = \widehat{P}_i^1 - \widehat{E}_{i-1}^0$, $v_3 = \widehat{P}_i^1 - \widehat{E}_i^0$, $v_4 = \widehat{P}_i^1 - \widehat{P}_i^0$, and let $S_i = \frac{1}{2}v_i \times v_{i+1}$, $T_i = \frac{1}{2}v_{i-1} \times v_{i+1}$, then

$$\beta_i^1 = \frac{2S_4}{2S_4 - T_1 + T_2 + \sqrt{D}}, \quad \beta_i^2 = \frac{2S_1}{2S_1 - T_1 - T_2 + \sqrt{D}}, \tag{14}$$

where $D = T_1^2 + T_2^2 + 2S_1S_3 + 2S_2S_4$.

The process of defining the subdivision matrix M for a n-sided face with knot intervals d_i, e_i, $i = 0, 1, \cdots, n-1$ is summarized as the following algorithm 3.3.

Algorithm 1 The algorithm to construct the subdivision matrix

Require: valence n, knot intervals d_i, e_i;
Ensure: The subdivision matrix M;

Define the eigen polygon to be a regular n-polygon;
Compute c_i according to Equation (8);
for $i = 0$ to $n-1$ **do**
  Compute β_i^1 and β_i^2 according to Equation (14);
end for
for $i = 0$ to $n-1$ **do**
  for $j = 0$ to $n-1$ **do**
    $M_{i,j} = (1-\beta_i^1)(1-\beta_i^2)\alpha_j\frac{e_{j+1}}{d_j+e_{j+1}}$
    $M_{i,j+1} = (1-\beta_i^1)(1-\beta_i^2)\alpha_j\frac{d_j}{d_j+e_{j+1}}$
  end for
  $M_{i,i-1} += \beta_i^1(1-\beta_i^2)\frac{e_i}{e_i+d_{i-1}}$
  $M_{i,i+1} += (1-\beta_i^1)\beta_i^2\frac{d_i}{e_{i+1}+d_i}$
  $M_{i,i} += \beta_i^1\beta_i^2 + \beta_i^1(1-\beta_i^2)\frac{d_{i-1}}{e_i+d_{i-1}} + (1-\beta_i^1)\beta_i^2\frac{e_{i+1}}{e_{i+1}+d_i}$
end for

Theorem 3.5 *If all the knot intervals are equal, then the present scheme will reduce to Catmull-Clark-variant Doo-sabin scheme. If the valence is four and the knot intervals satisfy the B-spline requirement, then the present scheme will reduce to non-uniform biquadratic B-spline refinement scheme.*

Proof If all the knot intervals are all equal, then $\alpha_i = \frac{1}{n}$ and

$$\widehat{V} = \sum_{i=0}^{n-1}\alpha_i\widehat{E}_i^0 = (0,0), \tag{15}$$

so we can verify that $\beta_i^1 = \beta_i^2 = \frac{1}{2}$ for all $0 \le i \le n-1$. In this case, the subdivision scheme is same as that of Catmull-Clark-variant Doo-sabin subdivision rule.

If $n = 4$ and the knot intervals satisfy the B-spline requirement, then

$$\widehat{V} = \sum_{i=0}^{3} \alpha_i \widehat{E}_i^0 = \left(\frac{d_0 - d_2}{d_0 + d_2}, \frac{d_1 - d_3}{d_1 + d_3} \right), \tag{16}$$

and $\beta_i^1 = \beta_i^2 = \frac{1}{2}$ for all $0 \le i \le 3$. So we can verify that the subdivision scheme is same as that of non-uniform biquadratic B-spline refinement rule. ∎

4 Result

While the subdivision matrix M is constructed only for a special planar polygon, but applying the matrix to arbitrary control meshes in R^3 yields better results. In this section, we analyze the convergence, continuity of the subdivision scheme and show the limit surfaces of three non-uniform Doo-Sabin subdivision schemes.

4.1 Convergence and Continuity Analysis

Firstly, we proved that our new non-uniform Doo-Sabin subdivision scheme is always convergent.

Theorem 4.1 *The non-uniform Doo-Sabin subdivision scheme in the present paper is always convergent.*

Proof Suppose the i-th row, j-th column element of the subdivision matrix M is $M_{i,j}$ and let the eigenvalues for the subdivision matrix M be $\lambda_k, k = 0, \cdots, n-1$, where $|\lambda_i| \le |\lambda_{i-1}|$. According to [38], the subdivision is convergent if and only if $\lambda_0 = 1$.

The proof includes two steps. First, we prove that for all i, $\beta_i^1, \beta_i^2 \in (0, 1)$. Actually, since $\widehat{P}^0$ is a regular n-polygon, and $\widehat{E}_i^0$ is the convex combination of $\widehat{P}_i^0$ and $\widehat{P}_{i+1}^0$, so n-polygon $\widehat{E}_0^0 \widehat{E}_1^0 \cdots \widehat{E}_{n-1}^0$ is a convex n-polygon. So $\widehat{V}$ is inside the n-polygon because it is the convex combination of all $\widehat{E}_i^0$. Thus, the quadrilateral $\widehat{V} \widehat{E}_{i-1}^0 \widehat{P}_i^0 \widehat{E}_i^0$ is a convex quadrilateral. As the point $\widehat{P}_i^1$ is in the interior of the quadrilateral, so there exist unique $\beta_i^1, \beta_i^2 \in (0, 1)$ satisfy Equation (13).

Now we prove that $\lambda_0 = 1$. Because $\sum_{j=0}^{n-1} M_{i,j} = 1, i = 0, 1, \cdots, n-1$, so 1 must be one of the eigenvalues. And $\beta_i^1, \beta_i^2 \in (0, 1)$, so $M_{i,j} > 0$. If $\lambda_0 > 1$, suppose $(v_0, \cdots, v_{n-1})$ is the corresponding eigenvector, and $v = \max_{i=0,\cdots,n-1}\{|v_i|\} \doteq |v_k|$, then

$$\begin{aligned} |\lambda_0 v_k| &= |\sum_{j=0}^{n-1} c_{k,j} v_j| \le \sum_{j=0}^{n-1} c_{k,j} |v_j| \\ &\le \sum_{j=0}^{n-1} c_{k,j} |v_k| = |v_k|, \end{aligned}$$

which is obvious not right. Thus, the new non-uniform Doo-Sabin subdivision scheme is convergent. ∎

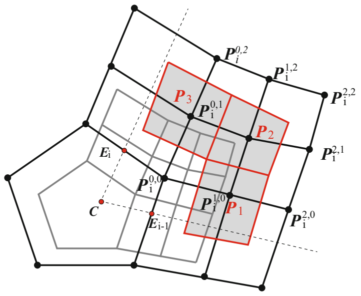

Figure 7 Part of the control points of the characteristic map

Theorem 4.2 *If the second and third eigenvalues for the subdivision matrix are λ, the limit surface of the new non-uniform Doo-Sabin subdivision scheme is G^1.*

Proof According to the construction of the subdivision scheme, it is obvious that $\lambda = \frac{1}{4} + \frac{1}{2}\cos^2(\frac{\pi}{n})$ must be the eigenvalue of the subdivision matrix M. If λ is the second and third eigenvalues, then in order to prove the limit surface is tangent continuous, we need to verify that the characteristic map exists and it is regular and injective[38]. To verify regularity and injectivity, we need to examine the characteristic map defined by three rings of control points. For a valence n face, referring to Figure 7, suppose the subdivision matrix of the three rings of control points is S_n, and let the control points for the characteristic map be $P_i^{j,k}$, $0 \le j, k \le 2$, $0 \le i \le n-1$. Denote $P_i = (\cos(\frac{2i\pi}{n}), \sin(\frac{2i\pi}{n})) \in R^2$, $i = 0, \cdots, n-1$, $E_i = \frac{d_i}{d_i + d_{i+2}} P_{i+1} + \frac{d_{i+2}}{d_i + d_{i+2}} P_i$, $C = \sum_{i=0}^{n-1} \alpha_i E_i$, then $M[P_0 - C, \cdots, P_{n-1} - C]^{\mathrm{T}} = \lambda[P_0 - C, \cdots, P_{n-1} - C]^{\mathrm{T}}$. Thus, we can set $P_i^{0,0} = P_i - C$.

For the points $P_{i-1}^{0,1}$ and $P_i^{1,0}$, according to the fact that the new grid after subdivision is the scale of λ of the given control grid. Using this relationship, we have

$$(P_i^{1,0} - P_i^{0,0})\lambda = \frac{3}{4}\frac{(2d_{i-1} + e_i)P_i^{0,0} + e_i P_{i-1}^{0,0}}{2(d_{i-1} + e_i)} - \lambda P_i^{0,0} - (1-\lambda)C + \frac{1}{4}\frac{(2d_{i-1} + e_i)P_i^{1,0} + e_i P_{i-1}^{0,1}}{2(d_{i-1} + e_i)}$$

$$(P_{i-1}^{0,1} - P_{i-1}^{0,0})\lambda = \frac{3}{4}\frac{d_{i-1}P_i^{0,0} + (d_{i-1} + 2e_i)P_{i-1}^{0,0}}{2(d_{i-1} + e_i)} - \lambda P_{i-1}^{0,0} - (1-\lambda)C + \frac{1}{4}\frac{d_{i-1}P_i^{1,0} + (d_{i-1} + 2e_i)P_{i-1}^{0,1}}{2(d_{i-1} + e_i)}.$$

Solving the linear systems we get

$$P_i^{1,0} - P_i^{0,0} = \frac{12\lambda}{(4\lambda - 1)(8\lambda - 1)}(E_{i-1} - C) - \frac{8\lambda - 4}{8\lambda - 1}(P_i^{0,0} - C),$$
$$P_{i-1}^{0,1} - P_{i-1}^{0,0} = \frac{12\lambda}{(4\lambda - 1)(8\lambda - 1)}(E_{i-1} - C) - \frac{8\lambda - 4}{8\lambda - 1}(P_{i-1}^{0,0} - C).$$

Similarly, we can compute $P_i^{2,0}$, $P_{i-1}^{0,2}$ as

$$P_i^{2,0} - P_i^{1,0} = \frac{6}{(4\lambda - 1)(8\lambda - 1)}(E_{i-1} - C) - \frac{2\lambda - 1}{\lambda(8\lambda - 1)}(P_i^{0,0} - C),$$
$$P_{i-1}^{0,2} - P_{i-1}^{0,1} = \frac{6}{(4\lambda - 1)(8\lambda - 1)}(E_{i-1} - C) - \frac{2\lambda - 1}{\lambda(8\lambda - 1)}(P_{i-1}^{0,0} - C).$$

Let $p_i = P_i^{0,0} - C$, $v_i = E_i - C$, then we compute the remaining control points $P_i^{j,k}$ such that $S_n[P_0^{0,0} - C, P_0^{1,0} - C, \cdots, P_{n-1}^{2,2} - C]^{\mathrm{T}} = \lambda[P_0^{0,0} - C, P_0^{1,0} - C, \cdots, P_{n-1}^{2,2} - C]^{\mathrm{T}}$. We obtain

$$\begin{aligned}
P_i^{1,1} &= \frac{9\left(32\lambda^2 - 4\lambda - 1\right)p_i + 36\lambda v_{i-1} + 36\lambda v_i}{(4\lambda-1)(8\lambda-1)(16\lambda-1)},\\
P_i^{2,1} &= \frac{3\left(32\lambda^2 + 44\lambda - 13\right)p_i + 108\lambda v_{i-1} + 6(2\lambda+1)v_i}{(4\lambda-1)(8\lambda-1)(16\lambda-1)},\\
P_i^{1,2} &= \frac{3\left(32\lambda^2 + 44\lambda - 13\right)p_i + 108\lambda v_i + 6(2\lambda+1)v_{i-1}}{(4\lambda-1)(8\lambda-1)(16\lambda-1)},\\
P_i^{2,2} &= \frac{(32\lambda^3 + 220\lambda^2 - 41\lambda - 4)p_i + 18\lambda(2\lambda+1)v_{i-1} + 18\lambda(2\lambda+1)v_i}{\lambda(4\lambda-1)(8\lambda-1)(16\lambda-1)}.
\end{aligned}$$

With all these control points, we can extract the Bézier control points for the patches P_1, P_2 and P_3 and compute the two directional derivatives of patch. For example, the two directional derivatives of patch P_2, $\frac{\partial P_2}{\partial t}$ and $\frac{\partial P_2}{\partial s}$, are bi-degree 2×1 and 1×2 Bézier patches respectively, where vectors of the control points are denoted as $T_{i,j}, 0 \le i \le 2, 0 \le j \le 1$ and $S_{i,j}, 0 \le i \le 1, 0 \le j \le 2$. We have

$$\begin{aligned}
S_{0,0} &= -\frac{2\left(-24\lambda^2 - 3\lambda\right)v_{i-1}}{(4\lambda-1)(8\lambda-1)(16\lambda-1)} - \frac{2\left(24\lambda^2 - 6\lambda\right)v_i}{(4\lambda-1)(8\lambda-1)(16\lambda-1)} - \frac{2\left(64\lambda^3 - 64\lambda^2 + 8\lambda + 1\right)p_i}{(4\lambda-1)(8\lambda-1)(16\lambda-1)}\\
S_{1,0} &= -\frac{\left(320\lambda^3 - 272\lambda^2 + 52\lambda - 1\right)p_i}{4\lambda(4\lambda-1)(8\lambda-1)(16\lambda-1)} + \frac{\left(512\lambda^3 + 256\lambda^2 + 16\lambda - 1\right)v_{i-1}}{16\lambda(4\lambda-1)(8\lambda-1)(16\lambda-1)} + \frac{3(1-4\lambda)v_i}{2(4\lambda-1)(8\lambda-1)(16\lambda-1)}\\
S_{0,1} &= \frac{6\left(8\lambda^2 + 2\lambda - 1\right)p_i}{(4\lambda-1)(8\lambda-1)(16\lambda-1)} + \frac{18\lambda v_{i-1}}{(4\lambda-1)(8\lambda-1)(16\lambda-1)} + \frac{24\lambda(1-4\lambda)v_i}{(4\lambda-1)(8\lambda-1)(16\lambda-1)}\\
S_{1,1} &= \frac{3\left(-32\lambda^2 + 28\lambda - 5\right)p_i}{(4\lambda-1)(8\lambda-1)(16\lambda-1)} + \frac{36\lambda v_{i-1}}{(4\lambda-1)(8\lambda-1)(16\lambda-1)} + \frac{3(1-4\lambda)v_i}{(4\lambda-1)(8\lambda-1)(16\lambda-1)}\\
S_{0,2} &= \frac{\left(192\lambda^2 + 24\lambda\right)v_{i-1}}{16\lambda(4\lambda-1)(8\lambda-1)(16\lambda-1)} + \frac{\left(128\lambda^3 + 112\lambda^2 - 32\lambda - 1\right)p_i}{4\lambda(4\lambda-1)(8\lambda-1)(16\lambda-1)} + \frac{\left(-2048\lambda^3 + 704\lambda^2 - 16\lambda + 1\right)v_i}{16\lambda(4\lambda-1)(8\lambda-1)(16\lambda-1)}\\
S_{1,2} &= \frac{\left(24\lambda^2 + 3\lambda\right)v_{i-1}}{\lambda(4\lambda-1)(8\lambda-1)(16\lambda-1)} + \frac{\left(6\lambda - 24\lambda^2\right)v_i}{\lambda(4\lambda-1)(8\lambda-1)(16\lambda-1)} + \frac{\left(-64\lambda^3 + 64\lambda^2 - 8\lambda - 1\right)p_i}{\lambda(4\lambda-1)(8\lambda-1)(16\lambda-1)}\\
T_{0,0} &= -\frac{2\left(64\lambda^3 - 64\lambda^2 + 8\lambda + 1\right)p_i}{(4\lambda-1)(8\lambda-1)(16\lambda-1)} - \frac{6\lambda(8\lambda-2)v_{i-1}}{(4\lambda-1)(8\lambda-1)(16\lambda-1)} + \frac{6\lambda(8\lambda+1)v_i}{(4\lambda-1)(8\lambda-1)(16\lambda-1)}\\
T_{1,0} &= \frac{6\left(8\lambda^2 + 2\lambda - 1\right)p_i}{(4\lambda-1)(8\lambda-1)(16\lambda-1)} + \frac{6\lambda(4-16\lambda)v_{i-1}}{(4\lambda-1)(8\lambda-1)(16\lambda-1)} + \frac{18\lambda v_i}{(4\lambda-1)(8\lambda-1)(16\lambda-1)}\\
T_{2,0} &= \frac{\left(128\lambda^3 + 112\lambda^2 - 32\lambda - 1\right)p_i}{4\lambda(4\lambda-1)(8\lambda-1)(16\lambda-1)} + \frac{\left(-2048\lambda^3 + 704\lambda^2 - 16\lambda + 1\right)v_{i-1}}{16\lambda(4\lambda-1)(8\lambda-1)(16\lambda-1)} + \frac{3(8\lambda+1)v_i}{2(4\lambda-1)(8\lambda-1)(16\lambda-1)}\\
T_{0,1} &= -\frac{\left(96\lambda^2 - 24\lambda\right)v_{i-1}}{16\lambda(4\lambda-1)(8\lambda-1)(16\lambda-1)} - \frac{\left(320\lambda^3 - 272\lambda^2 + 52\lambda - 1\right)p_i}{4\lambda(4\lambda-1)(8\lambda-1)(16\lambda-1)} - \frac{\left(-512\lambda^3 - 256\lambda^2 - 16\lambda + 1\right)v_i}{16\lambda(4\lambda-1)(8\lambda-1)(16\lambda-1)}\\
T_{1,1} &= \frac{3\left(-32\lambda^2 + 28\lambda - 5\right)p_i}{(4\lambda-1)(8\lambda-1)(16\lambda-1)} + \frac{3(1-4\lambda)v_{i-1}}{(4\lambda-1)(8\lambda-1)(16\lambda-1)} + \frac{36\lambda v_i}{(4\lambda-1)(8\lambda-1)(16\lambda-1)}\\
T_{2,1} &= \frac{\left(24\lambda^2 + 3\lambda\right)v_i}{\lambda(4\lambda-1)(8\lambda-1)(16\lambda-1)} + \frac{\left(-64\lambda^3 + 64\lambda^2 - 8\lambda - 1\right)p_i}{\lambda(4\lambda-1)(8\lambda-1)(16\lambda-1)} + \frac{3(2-8\lambda)v_{i-1}}{(4\lambda-1)(8\lambda-1)(16\lambda-1)}.
\end{aligned}$$

The control points for $\frac{\partial P_2}{\partial t}$ are convex combinations of vectors p_i, $-v_{i-1}$ and v_i, while the control points for $\frac{\partial P_2}{\partial s}$ are convex combinations of vectors p_i, v_{i-1} and $-v_i$, so the patch of P_2 is regular and injective. On the other hand, because C is a convex combination of the points E_i, we can observe that for any i, the points $P_i^{j,k}, 0 \leq j,k \leq 2$ lie in the regions bounded by two rays CE_{i-1} and CE_i. Thus, the characteristic map of the subdivision is regular and injective for any valence and any positive knot intervals, which concludes that the surface is G^1. ∎

It is much better if we can prove mathematically that the λ must be the second and third eigenvalues. However, we do not have an analytical proof for this. But we did a wild range of numerical tests. For each valence $n, 3 \leq n \leq 30$ faces, we generated a set of random knot intervals $d_i, e_i \in [1, 10^6]$, and preform three non-uniform subdivision scheme on the models. For each model, we calculate the eigenvalues verify that whether the second and third eigenvalues are the same. In all the million tests, λ is the second and third eigenvalue of subdivision matrix. In other words, according to Theorem 4.2, the limit surface in all these tests are G^1 continuous. The example characteristic maps of the new subdivision scheme for valence 3, 5, 6, 7, 8, 9 with non-uniform knot intervals are shown in Figure 8.

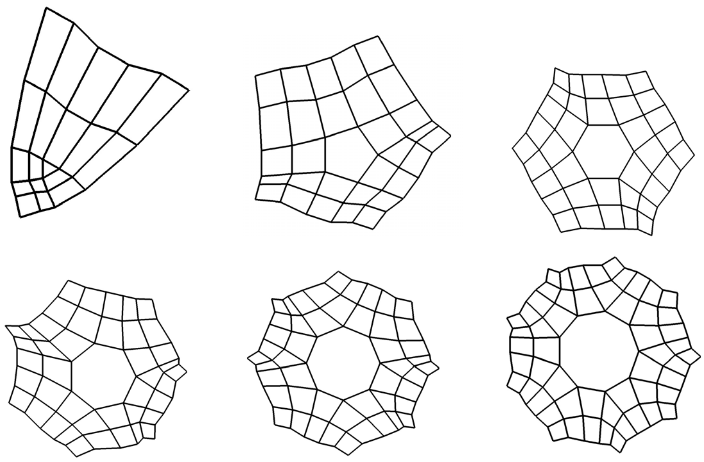

Figure 8 The example characteristic maps of the new subdivision scheme for valence 3 to 9 with non-uniform knot intervals

Similar numerical experiments have been done for NURDS scheme[33] and NURSS scheme[32]. We find that for $3 \leq n \leq 30$, the NURDS limit surface is G^1 continuity in the case of only one knot being different from the others. However, the scheme is only G^0 for almost all the other cases. For example, for the valence 3, if $\{d_i\} = \{9, 7, 2\}$ and $\{e_i\} = \{6, 1, 5\}$ the limit surface is only G^0. For valence 5, if $\{d_i\} = \{6, 7, 3, 7, 7\}$ and $\{e_i\} = \{10, 4, 1, 5, 7\}$, the limit surface is also only G^0.

For quadratic NURSS scheme[32], the authors proved that eigenvalue satisfies the requirement for G^1 continuous when the valence n is less than 9. However, for higher valence, both [37] and [33] point out that quadratic NURSSes converge for $n \leq 12$, but may diverge when $n > 12$.

Our experiments find the similar result and we also find that in some cases, the scheme is convergent but the limit surface is only G^0. For example, in a valence 14 face, if we define the knot intervals $\{d_i\}$ to be {9718, 478, 5255, 4437, 1335, 1745, 1366, 3849, 1946, 8204, 294, 9208, 408, 1219} and $\{e_i\}$ to be {75, 1770, 9495, 4072, 6188, 924, 2280, 1454, 1852, 7743, 3283, 16, 7617, 387}, the limit surface is only G^0.

4.2 Limit Surfaces

In order to show the quality of our new subdivision scheme, we present some numerical experiments on our new scheme and compare them with two existing non-uniform Doo-Sabin subdivision methods (see Figures 9,13,14). We marked the knot intervals in the initial control grid in each example where all the non-marked knot intervals are ones. As in all our experiments, the NURSS scheme and NURDS scheme provide very similar quality limit surfaces, so in the following, we only show one of the limit surfaces. And in our experiments, all three subdivision schemes produce very similar result limit surfaces for valence three. However, our new subdivision scheme produces better shape quality for the rest valences.

Figure 9 shows the limit surfaces produced by NURSS and the new schemes for a valences five extraordinary face. The NURSS limit surface has unwanted creases as shown in Figure 9 (b). In additional, some points on the limit surface lie under the xy-plane. In other words, the NURSS scheme does not satisfy the convex hull property. Figure 9 (c) shows the limit surface generated by our new scheme which produces better limit surface. As all the elements for our subdivision matrix are non-negative, so our scheme satisfies the convex hull properties.

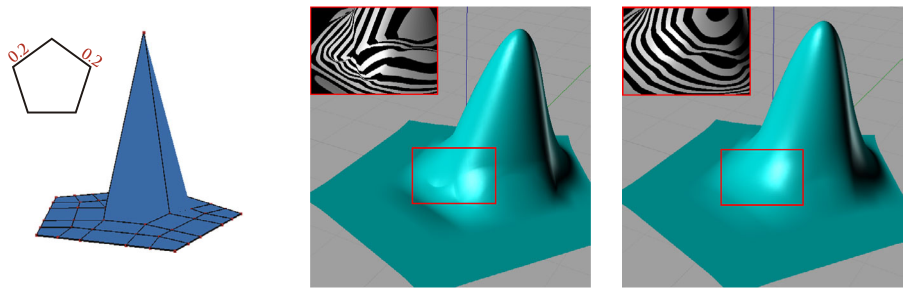

(a) Initial control grid (b) NURSS (c) The present scheme

Figure 9 Comparison of the limit surface of a valence five extraordinary face for NURSS scheme and our new subdivision scheme

Figures 10, 11, 12, 13 and 14 show the limit surfaces created by NURDS or NURSS scheme and our new scheme for valences six, seven, eight, nine extraordinary faces and a ring model. We can obverse the similar conclusion as well.

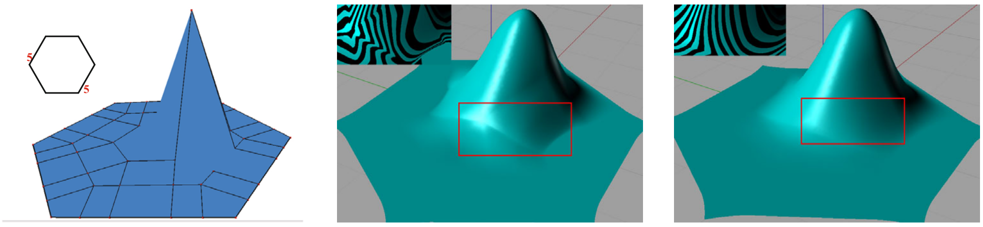

(a) Initial control grid (b) NURDS (c) The new scheme

Figure 10 Comparison of the limit surface of a valence six extraordinary face for NURDS scheme and our new subdivision scheme

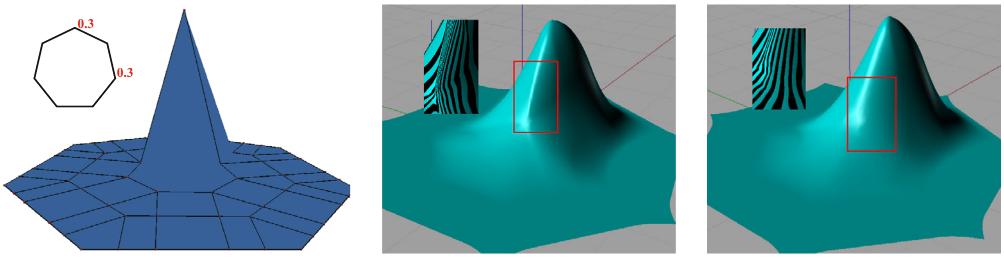

(a) Initial control grid (b) NURSS (c) The new scheme

Figure 11 Comparison of the limit surface of a valence seven extraordinary face for NURSS scheme and our new subdivision scheme

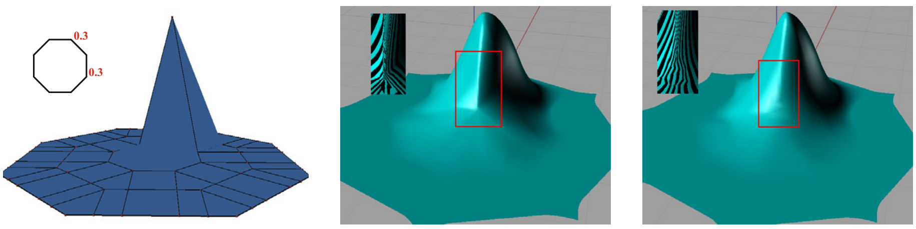

(a) Initial control grid (b) NURSS (c) The new scheme

Figure 12 Comparison of the limit surface of a valence eight extraordinary face for NURSS scheme and our new subdivision scheme

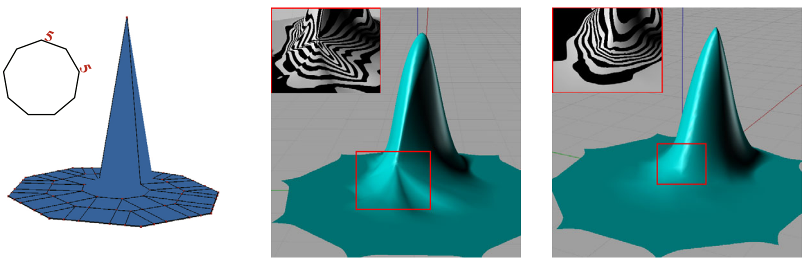

(a) Initial control grid (b) NURDS (c) The new scheme

Figure 13 Comparison of the limit surface of a valence nine extraordinary face for NURDS scheme and our new subdivision scheme

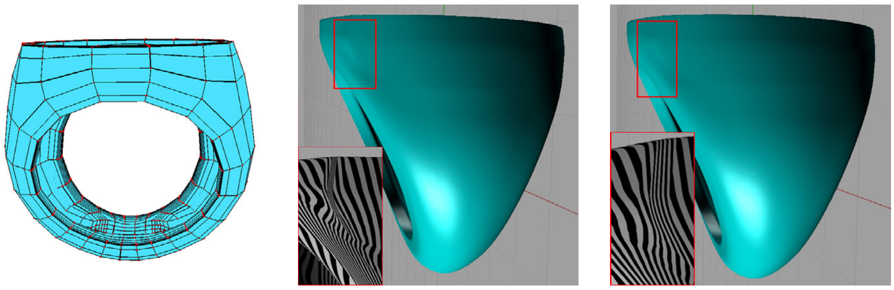

(a) Initial control grid (b) NURSS (c) The new scheme

Figure 14 Comparison of the limit surface of a ring model for NURSS scheme and our new subdivision scheme

5 Summary and Future Work

In this paper, the eigen polygon has been successfully implemented to construct a new non-uniform Doo-sabin subdivision scheme, which is a generalization of Catmull-Clark-variant Doo-Sabin subdivision scheme to non-uniform knot intervals and also a generalization of nonuniform biquadratic B-spline to arbitrary topology. This paper proved that the subdivision surfaces are always G^1 for any given random selecting knot intervals for all the valence between 3 and 30 if the subdivision matrix has two identical eigenvalues λ. Comparing the currently proposed scheme with the other two schemes we observe that our scheme gives better quality shape as shown in Figures 9, 13, 14.

There are many interesting problems to be further explored. For example, the eigen polygon idea has been applied to construct the subdivision scheme for odd degrees in [35] and even degrees in the present paper. The natural question is how to generalize the method to handle arbitrary degrees. There are some degrees of freedom to define the eigen polygon, so what is the behavior of the other eigen polygons? We don't have a mathematical proof for the subdivision surface is always G^1, and suggest that this is also an interesting problem for future directions.

References

[1] Warren J and Weimer H, *Subdivision Methods for Geometric Design*, Morgan, Kaufmann, 2002.

[2] Muller K, Reusche L, and Fellner D, Extended subdivision surfaces: Building a bridge between NURBS and Catmull-Clark surfaces, *ACM Transactions on Graphics*, 2006, **25**: 268–292.

[3] Doo D and Sabin M, Behaviour of recursive division surfaces near extraordinary points, *Computer Aided Design*, 1978, **10**: 356–360.

[4] Catmull E and Clark J, Recursively generated B-spline surfaces on arbitrary topological meshes, *Computer Aided Design*, 1978, **10**: 350–355.

[5] Loop C, Smooth subdivision surfaces based on triangles, Master's thesis, University of Utah, 1987.

[6] Kobbelt L, $\sqrt{3}$-subdivision, SIGGRAPH '00: Proceedings of the 27th annual conference on Computer graphics and interactive techniques, ACM Press/Addison-Wesley Publishing Co., 2000, 103–112.

[7] Velho L and Zorin D, Quasi 4-8 subdivision, *Computer Aided Geometric Design*, 2001, **18**: 345–358.

[8] Velho L and Zorin D, 4-8 subdivision, *Computer Aided Geometric Design*, 2001, **18**: 397–427.

[9] Stam J and Loop C, Quad/Triangle subdivision, *Computer Graphics Forum*, 2003, **22**: 1–7.

[10] Peters J and Shiue L, Combining 4- and 3-direction subdivision, *ACM Transactions on Graphics*, 2004, **23**: 980–1003.

[11] Dyn N, Levin D, and Gregory J A, A four-point interpolatory subdivision scheme for curve design, *Computer Aided Geometric Design*, 1987, **4**: 257–268.

[12] Dyn N and Levin D, A butterfly subdivision scheme for surface interpolation with tension control, *ACM Transactions on Graphics*, 1990, **9**: 160–169.

[13] Zorin D, Schröder P, and Sweldens W, Interpolating Subdivision for meshes with arbitrary topology, *SIGGRAPH'96: Proceedings of the 23rd Annual Conference on Computer Graphics and Interactive Techniques*, ACM, New York, NY, USA, 1996, 189–192.

[14] Kobbelt L, Interpolatory subdivision on open quadrilateral nets with arbitrary topology, *Computer Graphics Forum*, 1996, **15**: 400–410.

[15] Deng C and Ma W, A unified interpolatory subdivision scheme for quadrilateral meshes, *ACM Transactions on Graphics*, 2013, **32**(3): 1–11.

[16] Li X and Zheng J, An alternative method for constructing interpolatory subdivision from approximating subdivision, *Computer Aided Geometric Design*, 2012, **29**(4): 474–484.

[17] Labsik U and Greiner G, Interpolatory $\sqrt{3}$ subdivision, *Computer Graphics Forum*, 2000, **19**: 131–138.

[18] Li G, Ma W, and Bao H, Interpolatory $\sqrt{2}$-subdivision surfaces, *Proc. Geometric Modeling and Processing*, 2004, 185–194.

[19] Beccari C, Casciola G, and Romani L, A unified framework for interpolating and approximating univariate subdivision, *Applied Mathematics and Computation*, 2010, **216**: 1169–1180.

[20] Luo Z and Qi W, On interpolatory subdivision from approximating subdivision scheme, *Applied Mathematics and Computation*, 2013, **220**: 339–349.

[21] Albrechta G and Romani L, Convexity preserving interpolatory subdivision with conic precision, *Applied Mathematics and Computation*, 2012, **219**(8): 4049–4066.

[22] Luo Z and Qi W, On interpolatory subdivision from approximating subdivision scheme, *Applied Mathematics and Computation*, 2013, **220**(1): 339–349.

[23] Cirak F, Ortiz M, and Schröder P, Subdivision surfaces: A new paradigm for thin shell analysis, *International Journal of Numerical Methods in Engineering*, 2000, **47**: 2039–2072.

[24] Burckhart D, Hamann B, and Umlauf G, Iso-geometric finite element analysis based on Catmull-Clark subdivision solids, *Computer Graphics Forum*, 2010, **29**(5): 1575–1584.

[25] Dikici E, Snare S R, and Orderud F, Isoparametric finite element analysis for Doo-Sabin subdivision models, *Proceedings of Graphics Interface*, 2012, 19–26.

[26] Yuan X and Tang K, Rectified unstructured T-splines with dynamic weighted refinement for improvement in geometric consistency and approximation convergence, *Computer Methods in Applied Mechanics and Engineering*, 2017, **316**: 373–399.

[27] Riffnaller-Schiefer A, Augsdorfera U, and Fellner D, Isogeometric shell analysis with NURBS

compatible subdivision surfaces, *Applied Mathematics and Computation*, 2016, **272**(1): 139–147.

[28] Wei X, Zhang Y, Hughes T J, et al., Truncated hierarchical Catmull-Clark subdivision with local refinement, *Computer Methods in Applied Mechanics and Engineering*, 2015, **291**: 1–20.

[29] Wei X, Zhang Y, Hughes T J R, et al., Extended truncated hierarchical Catmull-Clark subdivision, *Computer Methods in Applied Mechanics and Engineering*, 2016, **299**: 316–336.

[30] Kang H, Li X, Deng J, et al., Truncated hierarchical Loop subdivision surfaces and application in isogeometric analysis, *Computers and Mathematics with Applications*, 2016, **72**: 2041–2055.

[31] Cashman T J, Augsdörfer U H, Dodgson N A, et al., NURBS with extraordinary points: High-degree, non-uniform, rational subdivision schemes, *ACM Transactions on Graphics*, 2009, **28**(3): 1–9.

[32] Sederberg T, Zheng J, Sewell D, et al., *Non-uniform Recursive Subdivision Surfaces*, SIGGRAPH'98, 1998, 387–394.

[33] Huang Z and Wang G, Non-uniform recursive Doo-Sabin surfaces, *Computer-Aided Design*, 2013, **43**: 1527–1533.

[34] Muller K, Funfzig C, Reusche L, et al., DINUS-double insertion, non-uniform, stationary subdivision surfaces, *ACM Transactions on Graphics*, 2010, **29**: 1–21.

[35] Li X, Finnigin T, and Sederberg T W, G^1 non-uniform Catmull-Clark surfaces, *ACM Transactions on Graphics*, 2016, **35**: 1–8.

[36] Li X and Chang Y, Non-uniform interpolatory subdivision surface, *Applied Mathematics and Computation*, 2018, **274**: 239–253.

[37] Qin K and Wang H, Eigenanalysis and continuity of non-uniform doo-sabin surfaces, *Proceedings of the 7th Pacific Conference on Computer Graphics and Applications*, 1999, 179–186.

[38] Peters J and Reif U, *Subdivision Surfaces*, Springer, 2008.